H1106 Journal of The Electrochemical Society, **157** (12) H1106-H1109 (2010)
0013-4651/2010/157(12)/H1106/4/$28.00 © The Electrochemical Society

Characterization of n-GaN with Naturally Textured Surface for Photoelectrochemical Hydrogen Generation

Shu-Yen Liu,[a] J. K. Sheu,[a,z] Jhao-Cheng Ye,[a] S. J. Tu,[a] Che-Kang Hsu,[a] M. L. Lee,[b,z] C. H. Kuo,[c] and W. C. Lai[a]

[a]*Institute of Electro-Optical Science and Engineering, Advanced Optoelectronic Technology Center, Center for Micro/Nano Science and Technology, National Cheng Kung University, Tainan City 70101, Taiwan*
[b]*Department of Electro-Optical Engineering, Southern Taiwan University, Tainan County 71001, Taiwan*
[c]*Institute of Lighting and Energy Photonics, National Chiao Tung University, Hsinchu 300, Taiwan*

To reduce light reflection and enlarge the effective reaction surface area at the n-GaN/electrolyte interface, n-GaN epitaxial layers with naturally textured surface are utilized. The layers are combined with Cr/Au ohmic contacts on n-GaN to form working electrodes that generate hydrogen by direct photoelectrolysis of water. Although the surface reflection on the naturally textured n-GaN samples is lower than that on n-GaN epitaxial layers with flat surface, our results reveal that the photocurrent (I_{ph}) and gas generation rates (R_{gas}) obtained from the naturally rough n-GaN samples are lower than those from the flat samples. The results can be attributed to the fact that the rough n-GaN surface caused by dense surface pits leads to significant recombination of photogenerated carriers with charged defects; this occurs before carriers reach the ohmic contacts, thereby resulting in lower I_{ph} and R_{gas}. Related analyses have been performed and presented in this paper to initially explain the possible mechanism.
 [DOI: 10.1149/1.3499327]

Manuscript submitted June 11, 2010; revised manuscript received August 25, 2010. Published October 19, 2010.

The use of solar power to direct photoelectrolysis is a promising method for generating hydrogen from water.[1,2] Unlike oil, solar energy is a renewable energy source. Water, as a product of hydrogen burning, will not cause pollution and can return to the photoelectrolysis system via an appropriate feedback mechanism. Water photoelectrolysis that utilizes an illuminated semiconductor/electrolyte scheme is a potential technique for generating hydrogen. However, not all semiconductors can be developed as working electrodes to split water; certain conditions must be satisfied. For example, the conduction band-edge potential of the semiconductor material must be lower than that of the cathode-reduction half-reaction, and its valence band-edge potential must be higher than that of the anode-oxidation half-reaction.[1] Various types of semiconductors can satisfy these conditions. Lower bandgap semiconductors, such as InP, GaAs, and CdSe can absorb solar light more effectively. However, it has been reported that these materials easily corrode in acidic or alkaline solution.[3,4] Fortunately, the band-edge potential of $In_xGa_{1-x}N$ materials satisfies the above-mentioned condition for splitting water.[5,6] Moreover, the material is potentially resistant to aqueous solutions.[7] The bandgap can also vary from 3.4 to 0.7 eV once the content of In is modified, resulting in the production of a photoelectrochemical (PEC) cell that can fit the solar spectrum to enhance light absorption.[7]

GaN-based light emitting diodes (LEDs) have been proven that naturally formed textures on the p-GaN surface can minimize the reflection of internal light at the GaN/air interface and consequently enhance the light-extraction efficiency.[8] A similar concept that the GaN/sapphire-based PEC cells can be expected to lessen the reflection of incident light at the GaN/air interface and consequently enhance the photocurrent. However, these two cases have a substantial difference, which is the position of the active regions. For the GaN/sapphire-based LEDs, the active regions are positioned at the InGaN/GaN multiple quantum well (MQW) interfaces, while for the PEC cells, the regions are situated in the GaN/electrolyte interfaces. Therefore, structural defects on the surface layer would produce different effects on the devices' performance. In general, wet etching and/or dry etching techniques are employed to form a variety of textured surfaces on the GaN samples. However, the etching process can easily cause surface damage. To prevent surface damage on the etched n-GaN layers, the n-GaN epitaxial layers can be grown with a naturally roughed surface or on a selective masked area to reduce light reflection on the sample surface compared with the flat-surfaced n-GaN layers. Waki et al. have reported that patterned n-GaN epitaxial layer formed by selective area regrowth with metal stripes can be used to achieve direct photoelectrolysis of water and increase the working area.[5] This study uses n-GaN epitaxial layers with abundant, naturally formed pits on the surface combined with Cr/Au bilayer metals to form the working electrodes.[8,9] The surface pits are on a submicron scale; therefore, the reflectance of incident light at the GaN/electrolyte interface can be reduced. Further, GaN samples with textured surface must possess a larger effective working area than the samples with flat surface. Comparative analyses of spectral reflection, photoluminescence (PL), and electrical properties between the naturally roughed and flat n-GaN samples are performed to explain the origin of the results. One can thus select between the increase or decrease of light absorption or reflection on one hand and material quality on the other hand for the improvement of performance of GaN/sapphire-based PEC cells.

Experimental

Two types of n-GaN epitaxial layers were grown on sapphire substrate to fabricate the PEC cells. One had dense surface pits and another had a specular surface. With the exception of growth temperature, the growth parameters between these two n-GaN epitaxial layers were the same. In other words, the samples with surface pits were grown at a lower temperature (approximately 900°C) compared with the samples with flat surface, which were grown at a higher temperature (approximately 1000°C). The dense V-shaped surface pits of the former samples can be attributed to the small diffusion length of Ga atoms. The small diffusion length of Ga atoms prevents the substance from migrating to proper locations at low temperature. The growth conditions in detail had been reported in earlier studies.[10,11]

Subsequently, a bilayer metal of Cr (50 nm)/Au (250 nm) was deposited on the n-GaN epitaxial layers to form ohmic contact of the working electrodes. Samples with textured and flat surfaces are labeled as PEC-1 and PEC-2, respectively. A potentiostat (Autolab-PGSTAT128N) was employed to supply the external bias. The current density was measured to evaluate the electrical properties of the PEC cells. A 300 W Xe lamp was utilized as the light source and 1 mol/l NaCl was used as the electrolyte at room temperature. A Ag/AgCl reference electrode and a platinum (Pt) wire counter electrode were used to measure potential. The bias voltage was applied to the working electrode with respect to the Ag/AgCl reference electrode. Hydrogen gas was generated at the Pt wire counter elec-

[z] E-mail: jksheu@mail.ncku.edu.tw; minglun@mail.stut.edu.tw

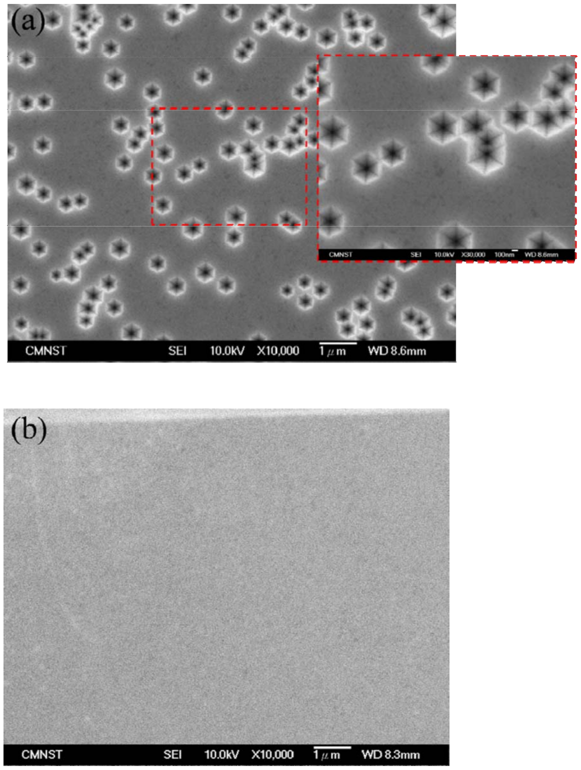

Figure 1. (Color online) The typical SEM images taken from the samples. (a) shows a plurality of V-shape pits on the surface of the sample PEC-1. The inset shows an enlarged inspection of a V-shaped pit which has a submicrometer scale. (b) shows the SEM image taken from the sample PEC-2.

trode. Gases were collected over water and a gas chromatograph (Agilent-6850) was used to determine the composition of the generated gases. Reflection spectra and room-temperature photoluminescence measurements were also performed to determine the reflectivity and crystal quality of the samples, respectively.

Results and Discussion

Figure 1 illustrates the typical scanning electron microscopy (SEM) images obtained from the samples. Figure 1a exhibits dense V-shaped pits on the surface, while Fig. 1b presents the SEM image obtained from the flat sample. In principle, the oblique facets of the V-shaped pits should be beneficial for light trapping and increasing effective reaction area. Figure 2 presents the reflection spectra obtained from the surfaces of the n-GaN layers. The naturally textured sample possesses lower reflectivity when the incident light wavelengths are shorter than 365 nm. This phenomenon can be attributed to the fact that n-GaN layers consisting of dense V-shaped pits on the surface can result in a better light trapping effect compared with the samples with flat surface. Theoretically, the PEC-1 is expected to produce higher photocurrent compared with the PEC-2. However, the experimental results are inconsistent with expectations.

Figure 3 demonstrates the photocurrent densities of PEC-1 and PEC-2 as a function of external bias voltage (V_{ext}). The photocurrent density of PEC-1, being markedly lower than PEC-2, suggests the negative effect arising from material defects in PEC-1, which will counteract the contribution of enhanced light trapping effect and increased effective work area. The formation of V-shaped pits appears to be a result of surface termination of dislocations,[8] which occurs along the growth direction, owing to a large lattice mismatch between the GaN and the sapphire. On the other hand, it has been suggested that acceptorlike states exist in the vicinity of dislocations and are responsible for the locally high reverse leakage current in GaN Schottky barrier diodes.[12] The charged defects will affect the carrier transport via scattering and/or recombine with the photogenerated carriers. This results in degradation of the photocurrent and gas generation rates.

Figure 4 displays the room-temperature photoluminescence spectra obtained from the samples. The yellow luminescence can be observed from the n-GaN with naturally textured surface. The PL result implies that the material quality of PEC-2 is better than that of PEC-1, which is consistent with the observation based on the mi-

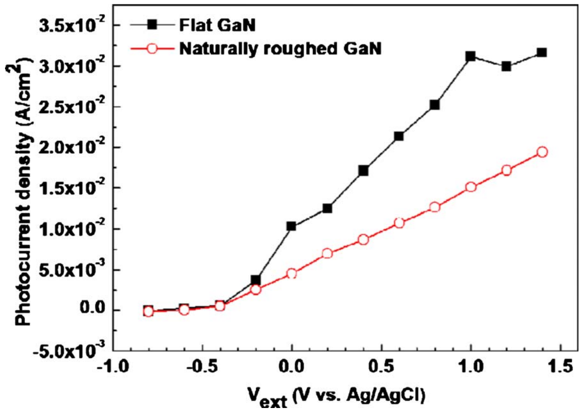

Figure 3. (Color online) Typical current–potential curves of PEC-1 and PEC-2.

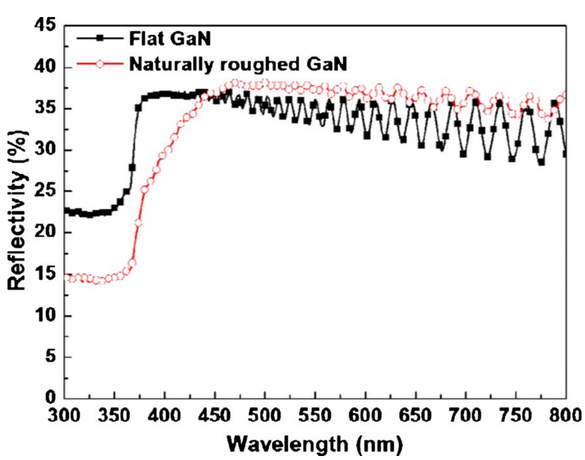

Figure 2. (Color online) The reflection spectra taken from the surfaces of the n-GaN layers.

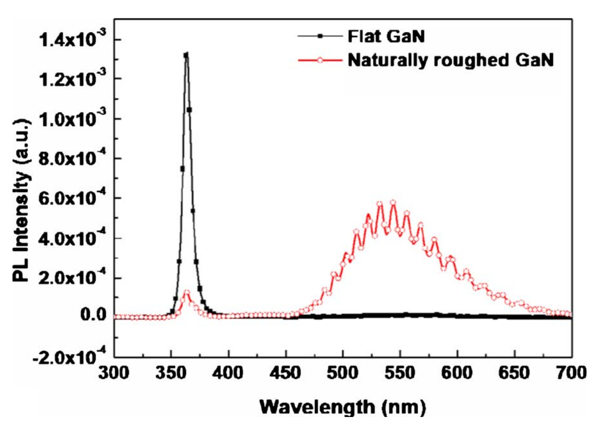

Figure 4. (Color online) The room-temperature PL spectra taken from the samples.

croscopy images in Fig. 1. In other words, the dislocation-related surface pits, which are formed by low-temperature epitaxial growth, may contain a number of defect states contributing to the yellow emission. It has been reported that the sources of yellow emission from GaN epitaxial layers are either the dislocations at low-angle grain boundaries in the material or the point defects which nucleate at the dislocations.[13] The dislocation-related defects degrade both the optical property and the electrical property of the GaN samples. Figure 3, particularly the lower photocurrent density observed in the PEC-1, suggests that the photogenerated carriers significantly recombine with the dislocation-related charged states before they reach the ohmic contacts. Although the dislocation-related defect states generally exist in the GaN layers grown on sapphire, the defect density is strongly dependent on growth conditions.

The initial motivation of this study is to create an n-GaN with naturally textured surface to enhance the light trapping effect and expand the effective reaction area at the GaN/electrolyte interface to increase the photocurrent in the PEC cells. However, experimental results indicate that the positive effect from samples with naturally textured surface is leveled off by the recombination of the photogenerated carriers and the dislocation-related states, which is different from the result from GaN-based LEDs. Moreover, light-extraction efficiency can be significantly improved by adding natural textures to the p-GaN top layer.[8] It has been extensively discussed and accepted that the InGaN-based blue/green LEDs' emission efficiency is weakly sensitive to structural defects density.[14] This is true even when the density is as high as 10^9–10^{10} cm^{-2}, which is six orders of magnitude higher than conventional AlGaAs or AlGaInP LEDs. A popular model has been proposed to explain why the highly defective InGaN materials can exhibit defect-insensitive emission characteristics. The presence of InN-rich or pure InN clusters in InGaN quantum well assumes the role of quantum dot-like localized states to confine the injected electron-hole pairs, which have recombined radiatively without diffusing toward the dislocations.[15]

In the PEC devices, the photogenerated carriers in the n-GaN layers need to diffuse away from the defects to reduce the probability of recombination before they reach the ohmic contact electrodes and external circuit. However, the screening of carriers in the local bandgap variation is absent because of the lack of indium fluctuation.[15] For an InGaN-based emitter with high indium content, the injected carriers can quickly and easily reach the active layer, owing to the external bias field. They can then spread into the localized bandgap minimum formed by In-rich clusters to prevent the carriers from recombining with the defects.[15] In contrast to the InGaN-based LEDs, the driving force of photogenerated carriers in the PEC devices diffusing to electrodes relies on the weak built-in fields resulting from the GaN/electrolyte junction or spatial distribution of carriers. Therefore, a GaN-based PEC device without InN-related localized bandgap minimum in the absorption layers is considered to be sensitive to structural defects. In other words, structural defects play the role of carrier killer in the PEC devices. Edge dislocations in n-GaN are suggested to be negatively charged,[12,16] while the low transverse mobility in GaN is proposed to have been caused by the scattering of electrons at charged dislocation lines. Filled traps along threading dislocation lines serve as coulomb scattering centers.[17] For vertical devices such as LEDs, the effect of scattering of electrons at threading dislocation lines must be more minor than that of lateral devices, such as field-effect transistors.[17] However, for the PEC devices in this study, the photogenerated electrons are transported laterally before being collected by the ohmic contact electrodes. Therefore, scattering by the charged dislocation lines will result in a reduction of electron mobility, thereby reducing the diffusion length. As a result, the photocurrent density of PEC-1 is markedly lower than that of PEC-2, even if the PEC-1 has a lower light reflection, as illustrated in Fig. 2 and 3. Moreover, the gas generation rates at zero external bias for PEC-1 and PEC-2 are 2.1 and 4.5 cm^3/hr, respectively, which are consistent with the photocurrent density obtained from these PEC devices.

In addition to the issue of carrier mobility, the flatband potential for application of PEC devices in water splitting reaction[18] is equally important. In this study, the flatband potential of PEC cells with the naturally roughed or flat n-GaN as the working electrodes was evaluated by Mott–Schottky plots. This method involves measuring the apparent capacitance as a function of applied potential under depletion condition. Subsequently, the flatband potential can be extracted based on the Mott–Schottky relationship[18]

$$\frac{1}{C_{sc}^2} = \frac{2}{e\varepsilon\varepsilon_0 N}\left(E - E_{FB} - \frac{kT}{e}\right) \qquad [1]$$

where C_{sc} is the capacitance of the space charge region, ε is dielectric constant of the semiconductor, ε_0 is permittivity of free space, N is donor density for an n-type semiconductor, E is the applied potential, and E_{FB} is the flatband potential. For a given semiconductor and electrolyte, there exists a unique potential drop between the surface and the neutral bulk region. The unique potential refers to the flatband potential of E_{FB}. To extract the E_{FB}, one has to use an equivalent circuit to fit the experimental data and then derive the capacitance values at the different applied potential.[19] Figure 5 shows the typical Mott–Schottky plots taken from the PEC-1 and PEC-2 in the dark. According to the Mott–Schottky plots, the E_{FB} value of PEC-1 and PEC-2 are −0.85 and −0.91 V, respectively. Considering the energy band diagram at the n-GaN/NaCl electrolyte interface, a large and negative E_{FB} is desirable because large E_{FB} means that a large built-in field near the n-GaN/NaCl electrolyte interface can prompt the photogenerated electrons drifting to ohmic contacts (Cr/Au). In other words, the large E_{FB} will enable photogenerated electrons to have small transit time before they reach the Pt electrode to generate hydrogen. Carrier transport will be dominated by diffusion if the E_{FB} is relatively small. Owing to this, the photocurrent strongly depends on material quality because photogenerated electrons might recombine with defect states before they reach the Pt electrode.[18] Experimental results indicate that the E_{FB} extracted from the Mott–Schottky plots is consistent with the measured current–potential curves of PEC-1 and PEC-2, as illustrated in Fig. 3 and 5. In fact, a smaller E_{FB} should, in principle, corresponds to a lower surface carrier concentration (i.e., a smaller energy difference between Fermi level and conduction band edge). PEC-1 with naturally roughed surface should have different surface states compared with the PEC-2 with flat surface. In other words, negatively charged dislocations in the naturally roughed n-GaN samples lead to a substantial compensation between free carriers and the defect-related charged states. This results in a reduction of surface carrier concentration. Therefore, the lower photocurrent and gas generation rates observed from the PEC-1 could give an edification that one should make a compromise between the light trapping and the material quality in the GaN-based PEC systems for enhancing their conversion efficiencies.

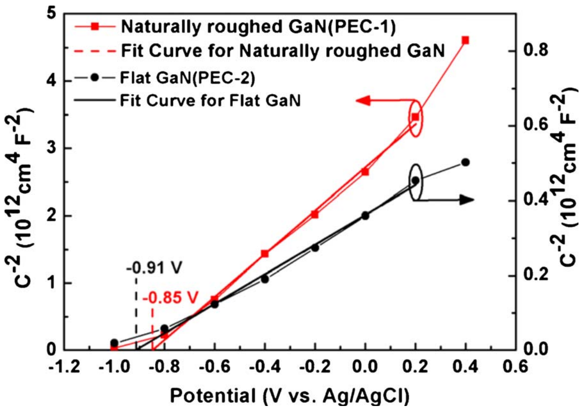

Figure 5. (Color online) The Mott–Schottky plots for naturally roughed and flat n-GaN samples in the dark and in 1 M NaCl electrolyte.

Conclusions

In summary, the motivation of this study was to utilize GaN PEC cells featuring dense V-shaped pits on the surface to reduce light reflection and to increase the effective reaction area at the GaN/electrolyte interface. However, experimental results indicate that the photocurrent (I_{ph}) and gas generation rate (R_{gas}) obtained from the naturally roughed n-GaN samples were lower than those of the flat samples. The positive effect of PEC cells on the naturally textured surface has been observed to be leveled off by the increased dislocation-related defects. In addition to the issue that carrier mobility will be reduced by scattering,[16] defect-related surface states have been shown to affect the E_{FB}. The formation of V-shaped surface pits grown at a relatively low temperature will inevitably intensify the generation of dislocation-related defects. Since the inherent properties of high-defect density in the GaN/sapphire-based materials are difficult to overcome, it is possible to increase the efficiency of GaN-based PEC devices by naturally texturing the sample surface and by passivating defects either during the material growth or post-treatment.

Acknowledgments

This work has been granted by Frontier Materials and Micro/Nano Science and Technology Center, NCKU. The authors would also like to acknowledge the National Science Council for the financial support and provision of the research grant NSC 97-2221-E-006-242-MY3 and 98-2221-E-218-005-MY3.

National Cheng-Kung University assisted in meeting the publication costs of this article.

References

1. A. J. Nozik and R. Memming, *J. Phys. Chem.*, **100**, 13061 (1996).
2. J. A. Turner, *Science*, **285**, 687 (1999).
3. A. J. Nozik, *J. Cryst. Growth*, **39**, 200 (1977).
4. R. C. Kainthla, B. Zelenay, and J. O'M. Bockris, *J. Electrochem. Soc.*, **134**, 841 (1987).
5. I. Waki, D. Cohen, R. Lal, U. Mishra, S. P. DenBaars, and S. Nakamura, *Appl. Phys. Lett.*, **91**, 093519 (2007).
6. J. Li, J. Y. Lin, and H. X. Jiang, *Appl. Phys. Lett.*, **93**, 162107 (2008).
7. J. Wu, W. Walukiewicz, K. M. Yu, J. W. Ager III, E. E. Haller, H. Lu, and W. J. Schaff, *Appl. Phys. Lett.*, **80**, 4741 (2002).
8. C. M. Tsai, J. K. Sheu, P. T. Wang, W. C. Lai, S. C. Shei, S. J. Chang, C. H. Kuo, C. W. Kuo, and Y. K. Su, *IEEE Photon. Technol. Lett.*, **18**, 1213 (2006).
9. M. L. Lee, J. K. Sheu, and C. C. Hu, *Appl. Phys. Lett.*, **91**, 182106 (2007).
10. C. M. Tsai, J. K. Sheu, W. C. Lai, Y. P. Hsu, P. T. Wang, C. T. Kuo, C. W. Kuo, S. J. Chang, and Y. K. Su, *IEEE Electron Device Lett.*, **26**, 464 (2005).
11. L. W. Wu, S. J. Chang, Y. K. Su, R. W. Chuang, Y. P. Hsu, C. H. Kuo, W. C. Lai, T. C. Wen, J. M. Tsai, and J. K. Sheu, *Solid-State Electron.*, **47**, 2027 (2003).
12. J. K. Sheu, M. L. Lee, and W. C. Lai, *Appl. Phys. Lett.*, **86**, 052103 (2005).
13. F. A. Ponce, D. P. Bour, W. Gotz, and P. J. Wright, *Appl. Phys. Lett.*, **68**, 57 (1996).
14. S. D. Lester, F. A. Ponce, M. G. Craford, and D. A. Steigerwald, *Appl. Phys. Lett.*, **66**, 1249 (1995).
15. S. Nakamura, *Science*, **281**, 956 (1998).
16. D. Cherns and C. G. Jiao, *Phys. Rev. Lett.*, **87**, 205504 (2001).
17. N. G. Weimann, L. F. Eastman, D. Doppalapudi, H. M. Ng, and T. D. Moustakas, *J. Appl. Phys.*, **83**, 3656 (1998).
18. M. Radecka, M. Rekas, A. Trenczek-Zajac, and K. Zakrzewska, *J. Power Sources*, **181**, 46 (2008).
19. M. Ono, K. Fujii, T. Ito, Y. Iwaki, A. Hirako, T. Yao, and K. Ohkawa, *J. Chem. Phys.*, **126**, 054708 (2007).